www.arpnjournals.com

PRESSURE AND PRESSURE DERIVATIVE ANALYSIS FOR A THREE-REGION COMPOSITE RESERVOIR

Freddy-Humberto Escobar, Javier-Andrés Martinez and Luis-Fernando Bonilla
Universidad Surcolombiana, Av. Pastrana, Neiva, Huila, Colombia
E-Mail: fescobar@usco.edu.co

ABSTRACT

In recent years, the constant increase in oil prices and declining reserves of conventional crude has changed the exploitation of deposits that were economically unattractive to be produced as an alternative way to keep the world's oil supply. Heavy oil deposits are mainly characterized by having high resistance to flow (high viscosity), which makes then difficult to produce. Since oil viscosity is a property that is reduced by increasing the temperature, thermal recovery techniques, such as steam injection or in-situ combustion, have been converted over the years into the main tool for tertiary recovery of heavy oil. Usually, well tests from enhanced oil recovery projects, such as steam injection, in-situ combustion, and CO2 flooding projects, are analyzed using a radial, two-region composite reservoir model. However, a three-region model may be more appropriate in many cases since a transition zone may be developed. In this work, the use of an existing analytical solution for the transient pressure response of a well in a radial, three-region reservoir is applied to develop a methodology utilizing a pressure and pressure derivative plot is developed for three-region composite reservoirs so that mobility and the distance to the radial discontinues are estimated. The methodology was successfully verified by its application to synthetic examples.

Keywords: pressure, radial flow, storativity ratio, mobility, radial discontinuity.

INTRODUCTION

The determination of the swept volume in a thermal oil recovery process is of primary concern. Estimation of the swept volume at intermediate stages of the operation, either in-situ combustion or steam injection, makes the early economic evaluation of the field operations possible.

The pressure behavior of a composite reservoir has been extensively considered. Watenbarger and Ramey (1970) modeled a finite-thickness skin region as a composite system and obtained the pressure transient behavior for such systems using finite differences. Their solutions correspond to a range of mobility ratio varying from 0, 1 to 3, 6. Brown (1985) investigated pressure derivative behavior of composite reservoirs but they limited his study to mobility and storativity ratios in the order of 0, 4 to 2 and 0, 3 to 30, respectively.

Gates and Ramey (1978) showed that the fuel concentration of an in-situ combustion oil recovery is an important parameter, which can control the economic results of this kind of operation. It is shown that fuel concentration may be determined by a number of methods. The total fuel consumption may be divided by the swept volume to obtain field estimates of the fuel concentration.

As far as the field of well test interpretation is concerned, some few researches can be named. Satman *et al*. (1980) presented an analytical solution for a two-zone, infinitely large composite reservoir undergoing a thermal recovery process. They specified constant rate as the inner boundary condition and neglected wellbore storage effects. They used the conventional straight-line method as the interpretation technique.

A year later, Walsch *et al*. (1981) conducted an analysis of pressure fall-off testing using a simplistic model. They found a long transition zone between two semilog straight lines for the swept and unswept regions obeying a pseudosteady-state behavior. They calculated the swept zone volume using mean values of temperature and pressure by applying the conventional straight-line method.

Two-region composite reservoirs models have been used to analyze pressure transient data from enhanced oil recovery projects. Three-region composite reservoir models have been used less frequently to analyze well test from enhanced oil recovery projects. Ambastha and Ramey (1989) presented a review of methodologies used to interpret well test data from enhanced recovery projects along with several design and interpretation relationships developed from an analysis of a well test response for a well located in a two-region composite reservoir. An analytical solution in the Lap lace space for the transient pressure behavior of a well in a three-region composite reservoir has been presented by Onyekonwu (1985), and Barua and Horner (1987). To study the effects of an intermediate region on the deviation time method and the pseudo steady state method, an analytical solution for a three-region reservoir presented by Onyekonwu (1985) is useful. Ambastha and Ramey (1992) reported for the first time the analysis of the pressure derivative for the systems under discussion. Recently Escobar, Martínez and Bonilla (2011) presented a methodology to analyze the pressure and pressure derivative behavior for different mobility and diffusivity ratios without using type-curve matching to analyze well test under thermal recovery conditions.

In this work, the Onyekonwu model is used to generate the pressure and pressure derivative behavior for different mobility and diffusivity ratios so that a methodology without using type-curve matching to analyze well test under thermal recovery conditions is

www.arpnjournals.com

presented. This is the first analytical methodology available. The model does not take into account the compressibility effects due to the possible presence of gas phase from the combustion process.

THREE-REGION COMPOSITE RESERVOIR MODEL

Figure-1 shows an idealized three-zone model, Onyekonwu (1985). Region 1 is the swept volume. Region 2 is the transition zone and is the region of rapidly changing mobility. Region 3 represents the zone that contains low mobility fluid. Assumptions implicit in the development of the model include:

a) The formation is homogeneous, horizontal, and of uniform thickness.
b) Flow is radial, and gravity and capillary effects are negligible.
c) In the three regions, the fluid is considered to be of slight constant compressibility but the fluid mobility and compressibility may be different.
d) The pressure gradient in the reservoir is considered to be small.
e) Other assumptions inherent to Darcy's law.

The diffusivity equation in dimensionless form for the three regions can be written as follows:

For Region-1

$$\frac{\partial^2 P_{D1}}{\partial r_D{}^2} + \frac{1}{r_D}\frac{\partial P_{D1}}{\partial r_D} = \frac{\partial P_{D1}}{\partial t_D}, \text{ for } 1 \le r_D \le R_{D1} \qquad (1)$$

For Region-2

$$\frac{\partial^2 P_{D2}}{\partial r_D{}^2} + \frac{1}{r_D}\frac{\partial P_{D2}}{\partial r_D} = \eta_{12}\frac{\partial P_{D2}}{\partial t_D}, \text{ for } R_{D1} \le r_D \le R_{D2} \quad (2)$$

Where

$$\eta_{12} = \left(\frac{k}{\phi\mu c_t}\right)_1 \bigg/ \left(\frac{k}{\phi\mu c_t}\right)_2 \qquad (3)$$

For Region-3

$$\frac{\partial^2 P_{D3}}{\partial r_D{}^2} + \frac{1}{r_D}\frac{\partial P_{D3}}{\partial r_D} = \eta_{13}\frac{\partial P_{D3}}{\partial t_D}, \text{ for } R_{D2} \le r_D \le \infty \quad (4)$$

Where

$$\eta_{13} = \left(\frac{k}{\phi\mu c_t}\right)_1 \bigg/ \left(\frac{k}{\phi\mu c_t}\right)_3 \qquad (5)$$

The inner and outer boundary conditions are given as follows:

$$\frac{C_D dP_{wD}}{dt_D} - \left[\frac{\partial P_{D1}}{\partial r_D}\right]_{r_D=1} = 1 \qquad (6)$$

$$P_{wD} = P_{D1} - s\left[\frac{\partial P_{D1}}{\partial r_D}\right]_{r_D=1} \qquad (7)$$

$$\lim_{r_D \to \infty} P_{D3}\left(r_D, t_D\right) = 0 \qquad (8)$$

Equation (6) states that dimensionless wellbore unloading rate plus the dimensionless sand face flow rate equals the dimensionless surface flow rate. Equation (7) introduces a steady-state skin effect and thus, a pressure drop at the sand face which is proportional to the sand face flow rate. Equation (8) is a mathematical representation of an infinite system. The outer boundary conditions in dimensionless form are as follows:

$$P_{D1} = P_{D2} \qquad \text{at} \qquad r_D = R_{D1} \qquad (9)$$

$$P_{D2} = P_{D3} \qquad \text{at} \qquad r_D = R_{D2} \qquad (10)$$

Equations (9) and (10) state that there is pressure continuity at the discontinuous interfaces at R_{D1} and R_{D2}. Also there is continuity of flux at the interfaces which mathematically is given by:

$$\frac{\partial P_{D2}}{\partial r_D} = M_{12}\frac{\partial P_{D1}}{\partial r_D} \qquad \text{at} \quad r_D = R_{D1} \qquad (11)$$

$$\frac{\partial P_{D3}}{\partial r_D} = M_{23}\frac{\partial P_{D2}}{\partial r_D} \qquad \text{at} \quad r_D = R_{D2} \qquad (12)$$

The initial conditions which state that the pressure in the system was at an initial value P_i, are also represented in dimensionless form as follows:

$$P_{D1}(r_D, 0) = 0 \qquad 1 \le r_D \le R_{D1} \qquad (13)$$

$$P_{D2}(r_D, 0) = 0 \qquad R_{D1} \le r_D \le R_{D2} \qquad (14)$$

$$P_{D3}(r_D, 0) = 0 \qquad R_{D2} \le r_D \le \infty \qquad (15)$$

FUNDAMENTAL EQUATIONS

The dimensionless quantities used in this work as defined as:

$$P_D = \left(\frac{k_1 h}{141,2 q \mu_1 B} \right) \Delta P \qquad (16)$$

$$t_{DR1} = \left(\frac{0,0002637 k_1}{\phi_1 \mu_1 c_{t1} R_1^{\ 2}} \right) t \qquad (17)$$

$$t_{DR2} = \left(\frac{0,0002637 k_1}{\phi_1 \mu_1 c_{t1} R_2^{\ 2}} \right) t \qquad (18)$$

$$M_{12} = \frac{\lambda_1}{\lambda_2} = \frac{(k / \mu)_1}{(k / \mu)_2} \qquad (19)$$

$$M_{13} = \frac{\lambda_1}{\lambda_3} = \frac{(k / \mu)_1}{(k / \mu)_3} \qquad (20)$$

$$F_{S12} = \left(\frac{\phi_1 c_{t1}}{\phi_2 c_{t2}} \right) \qquad (21)$$

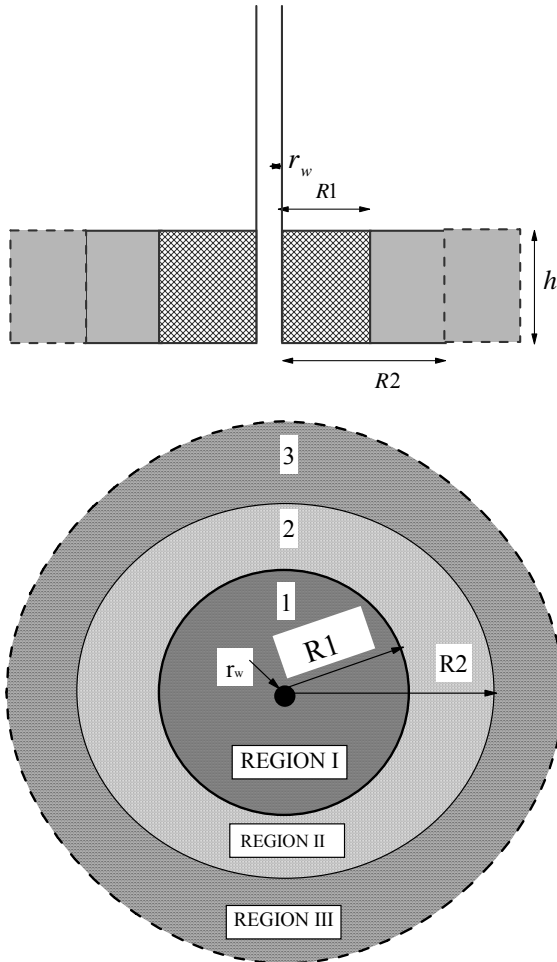$$F_{S13} = \left(\frac{\phi_1 c_{t1}}{\phi_3 c_{t3}} \right) \qquad (22)$$

EFFECT OF MOBILITY AND STORITIVITY RATIO

Figure-2 shows the effect of M_{12} on pressure derivative on pressure derivative behavior for a fixed F_{S12}, F_{S13}, M_{13} and R_2. As mobility between regions 1 and 2 increases, the pressure derivative goes through a first maximum value, while the latter remains almost constant until the relationship of the mobility ratios is equal to unity. The second radial flow is not visible due to the contrast in the properties between regions 2 and 3.
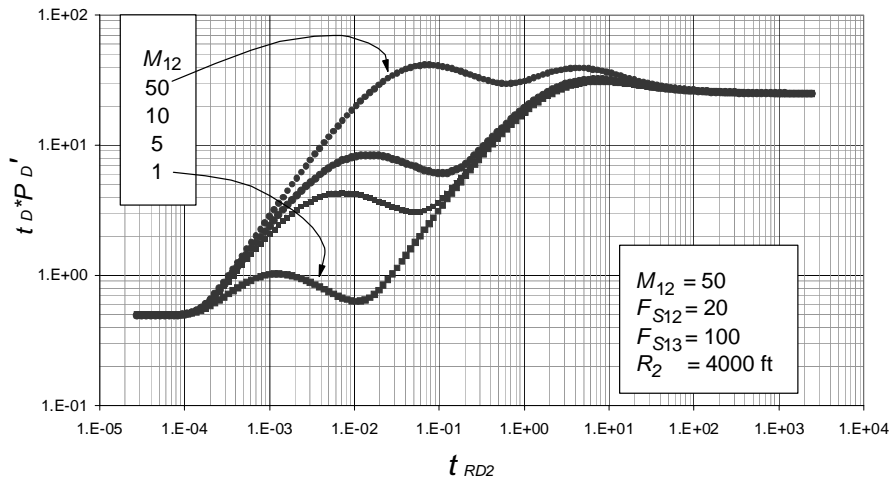

Figure-1. Three-zone model of the porous system.

Figure-2. Effect of mobility ratio between regions 1 and 2.

Figure-3 shows the effect of M_{13} on the pressure derivative behavior for fixed values of F_{S12}, F_{S13}, M_{12} and R_2. As mobility between regions 1 and 3 increases, the pressure derivative goes through a first maximum value which remains unaltered, while the latter increases its value.

Figure-4 shows the effect of F_{S12} on the pressure derivative behavior for fixed values of F_{S13}, M_{12}, M_{13} and R_2. As storativity ratio between regions 1 and 2 increases, the value of the maximum second derivative also increases and moves to the right-hand side.

Figure-5 shows the effect of Fs_{13} on the pressure derivative behavior for fixed values of F_{S12}, M_{12}, M_{13} and R_2. As storativity ratio between regions 1 and 3 increases,

the value of the maximum second derivative also increases, but the time of the second peak remains unaltered.

SWEPT REGION VOLUME AND DISCONTINUITY RADIUS OF THE INTERMEDIATE REGION

The permeability of the inner zone or swept region is found using the following equation, Tiab (1993):

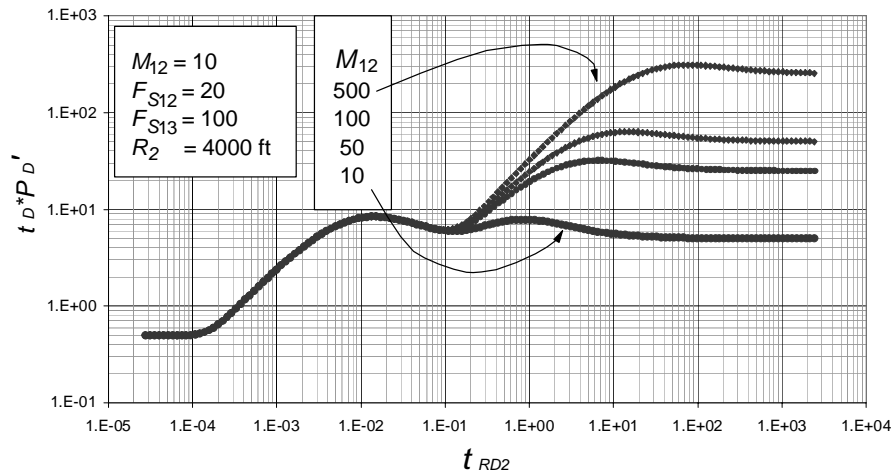$$k_1 = \frac{70,6 q_a \mu_1 B}{h (t * \Delta P')_{r1}} \tag{23}$$

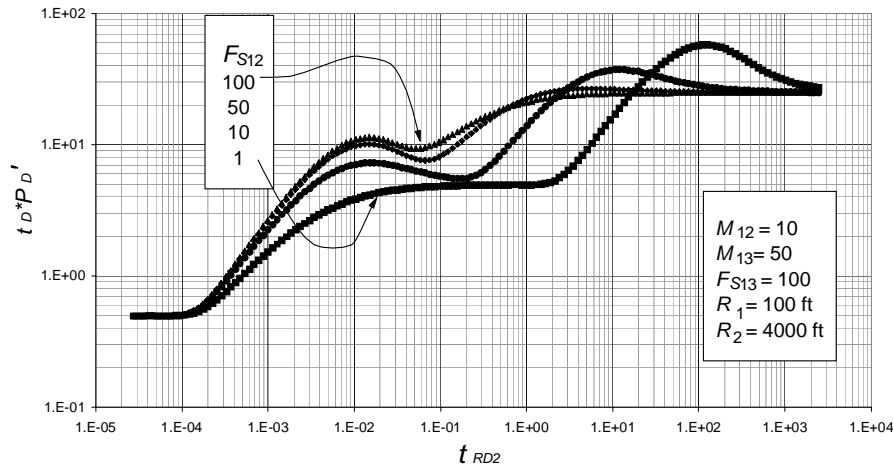**Figure-3.** Effect of mobility ratio between regions 1 and 3.

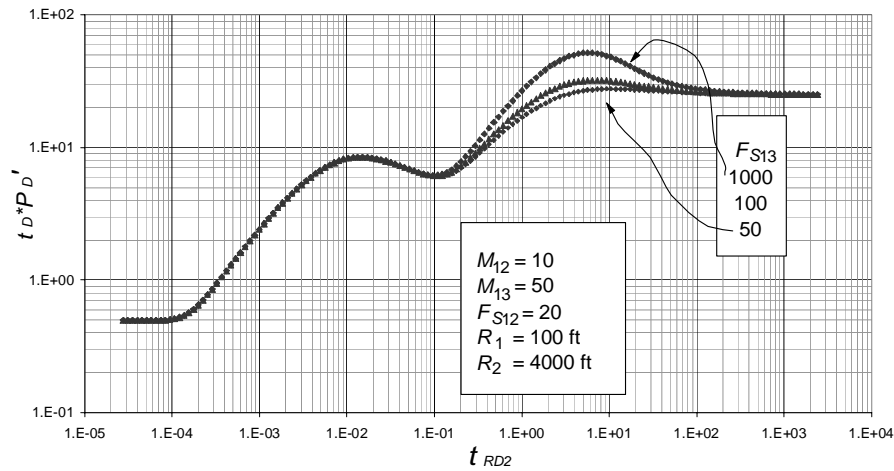**Figure-4.** Effect of storativity ratio between regions 1 and 2.

www.arpnjournals.com

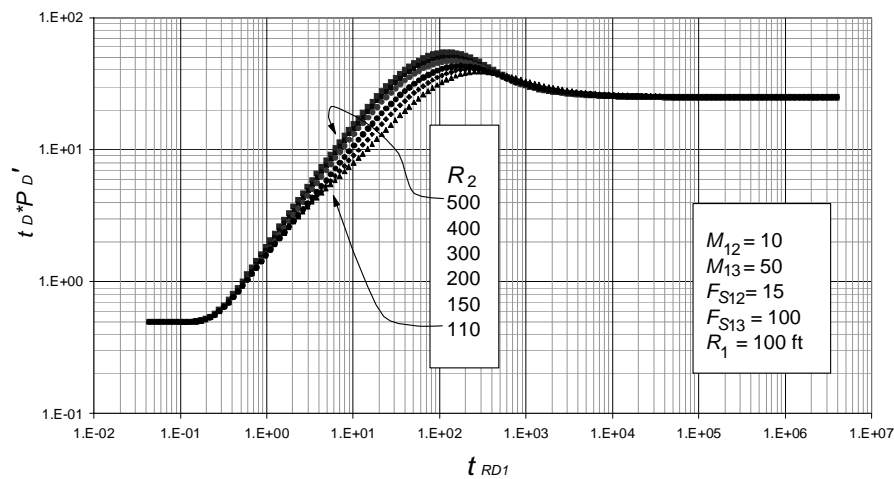**Figure-5.** Effect of storativity ratio between regions 1 and 3.

Figure-6. Effect of R_2 on pressure derivative with t_{DR1}.

The skin factor is found:

$$s = \frac{1}{2}\left(\frac{\Delta P_{r1}}{(t*\Delta P')_{r1}} - \ln\left(\frac{k_1 t_{r1}}{(\phi\mu c_t)_1\, r_w^{\,2}} \right) + 7,43 \right) \quad (24)$$

The radius of swept region is estimated with the end of first radial flow at $t_{RD1} = 0.18$ (See Figure-6).

$$R_1 = \sqrt{ \frac{0,001465 k_1 t_{er1}}{\mu_1 (\phi c_t)_1} } \quad (25)$$

The pressure derivative has a first maximum in the transition between the first and second region. The developed equations of dimensionless time at this point are:

$$(t_{RD})_{max1} = M12\big(2,76 - 0,276\log F_{S12}\big),\ \text{for } 1 < F_{S12} < 45$$
$$\text{and } R_2/R_1 > 15 \quad (26)$$

$$(t_{RD})_{max1} = M12\big(1,68 + 0,38\log F_{S12}\big),\ \text{for } F_{S12} \geq 45 \text{ and}$$
$$R_2/R_1 > 15 \quad (27)$$

Replacing the dimensionless terms in *Equations* 26 and 27, the mobility in the outer region according to the value of F_{s12} is given by:

$$\left(\frac{k}{\mu} \right)_2 = \frac{(\phi_1 c_{t1}) R_1^2}{0,0002637 t_{max1}} \left(2,76 - 0,276\log\left[\frac{\phi_1 c_{t1}}{\phi_2 c_{t2}} \right] \right) \quad (28)$$

$$\left(\frac{k}{\mu} \right)_2 = \frac{(\phi_1 c_{t1}) R_1^2}{0,0002637 t_{max1}} \left(1,68 + 0,38\log\left[\frac{\phi_1 c_{t1}}{\phi_2 c_{t2}} \right] \right) \quad (29)$$

The equation of the dimensionless pressure derivative at the first maximum point (peak), corrected by Ambastha and Ramey (1989) is:
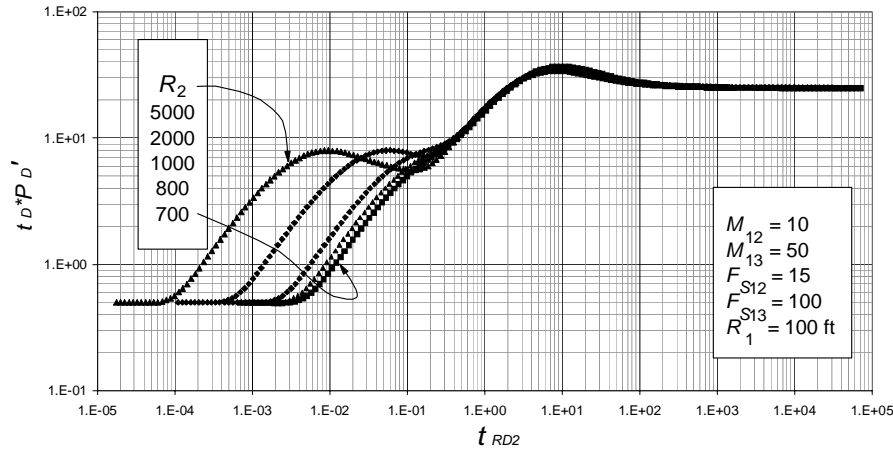

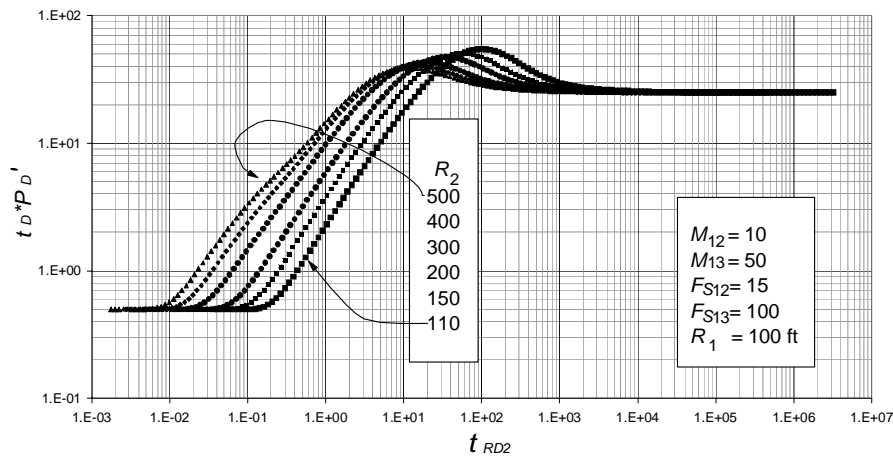**Figure-7.** Effect of R_2 on pressure derivative.

Figure-8. Effect of R_2 on pressure derivative.

$$\left(t_D * P_D{'}\right)_{max1} = M12\left(0,304 + 0,4343 \log F_{S12}\right)$$, for $M12 > 1$ and $R_2/R_1 > 15$ \hfill (30)

Replacing the dimensionless terms in Equation (30), it yields:

$$\left(\frac{k}{\mu}\right)_2 = \frac{141,2 q_a B}{h\left(t * \Delta P'\right)_{max1}}\left[0,304 + 0,4343 \log\left(\frac{\phi_1 c_{t1}}{\phi_2 c_{t2}}\right)\right] \quad (31)$$

Figure-7 shows when then relationship between the radius of the second region and the swept region is greater than or equal to 7. Two maxima are observed in the pressure derivative, and based on the value of t_{Dr2}, the second maximum remains constant. For $R_2/R_1 \geq 7$, the dimensionless pressure derivative of the second peak is estimated with:

$$\left(t_D * P_D\right)_{max2} = M13\left(-0,16077835 \ln\left(\frac{F_{S12}}{F_{S13}}\right) + 0,36060599\right) + M12\left(-0,034756599 \ln\left(\frac{F_{S12}}{F_{S13}}\right) + 0,10347416\right) \quad (32)$$

Replacing the dimensionless terms:

www.arpnjournals.com

$$\lambda_2 = \lambda_1 \frac{\left(-0,034756599\ln\left(\frac{F_{S12}}{F_{S13}}\right)+0,10347416\right)}{\left(t_D * P_D\right)_{\max 2} - \frac{\lambda_1}{\lambda_3}\left(-0,16077835\ln\left(\frac{F_{S12}}{F_{S13}}\right)+0,36060599\right)} \tag{33}$$

This is valid for $F_{S12}/F_{S13} \leq 0,4$. The dimensionless time of the second peak is estimated with:

$$\left(t_{DR2}\right)_{\max 2} = \frac{M13}{F_{S12}}\left[7,9020822\left(\frac{F_{S12}}{F_{S13}}\right)+1,5808639\right] + \frac{M12}{F_{S12}}\left[-10,9839962\left(\frac{F_{S12}}{F_{S13}}\right)+0,51691818\right] \tag{34}$$

Which is valid for $0,1 \leq F_{S12}/F_{S13} \leq 0,4$ when $M_{13}/M_{12} > 1$.

$$\left(t_{DR2}\right)_{\max 2} = \frac{M13}{F_{S12}}\left[-1,09372076\left(\frac{F_{S12}}{F_{S13}}\right)+2,4179022\right] - \frac{M12}{F_{S12}}\left[7,4853828\left(\frac{F_{S12}}{F_{S13}}\right)+0,085786786\right] \tag{35}$$

This is valid for $0,01 \leq F_{S12}/F_{S13} < 0,1$ and $0,1 \leq F_{S12}/F_{S13} \leq 0,4$ when $M_{13}/M_{12} = 1$. Replacing the dimensionless terms in Equations (34) and (35), the radius of second region according to the value of F_{S12}/F_{S13} is given by:

$$R_2 = \sqrt{\frac{\left(\frac{0,0002637\lambda_1 t_{\max 2}}{\phi_1 c_{t1}}\right)}{\frac{M13}{F_{S12}}\left[7,9020822\left(\frac{F_{S12}}{F_{S13}}\right)+1,5808639\right] + \frac{M12}{F_{S12}}\left[-10,9839962\left(\frac{F_{S12}}{F_{S13}}\right)+0,51691818\right]}} \tag{36}$$

$$R_2 = \sqrt{\frac{\left(\frac{0,0002637\lambda_1 t_{\max 2}}{\phi_1 c_{t1}}\right)}{\frac{M_{13}}{F_{S12}}\left[-1,09372076\left(\frac{F_{S12}}{F_{S13}}\right)+2,4179022\right] - \frac{M_{12}}{F_{S12}}\left[7,4853828\left(\frac{F_{S12}}{F_{S13}}\right)+0,085786786\right]}} \tag{37}$$

Figure-8 shows when then the relationship between the radius of the second region and the first region is less than 7. The pressure derivative behaves as a reservoir composed by two zones, being observed only the second maximum which is not constant.

If $R_2/R_1 < 7$ is not possible to determine the mobility of the second region, because it depends on all the variables studied since they are not kept constant. For $1,1 \leq R_2/R_1 < 3.5$ and $0,01 < F_{S12}/F_{S13} < 0,1$:

$$\frac{R_2}{R_1} = \frac{a + c\ln\left(\frac{t_{DR1\max}}{M13}\right) + e\left(\frac{F_{S12}}{F_{S13}}\right) + g\left(\ln\left(\frac{t_{DR1\max}}{M_{13}}\right)\right)^2 + i\left(\frac{F_{S12}}{F_{S13}}\right)^2 + k\left(\frac{F_{S12}}{F_{S13}}\right)\ln\left(\frac{t_{DR1\max}}{M_{13}}\right)}{1 + b\ln\left(\frac{t_{DR1\max}}{M13}\right) + d\left(\frac{F_{S12}}{F_{S13}}\right) + f\left(\ln\left(\frac{t_{DR1\max}}{M_{13}}\right)\right)^2 + h\left(\frac{F_{S12}}{F_{S13}}\right)^2 + j\left(\frac{F_{S12}}{F_{S13}}\right)\ln\left(\frac{t_{DR1\max}}{M_{13}}\right)} \tag{38}$$

For $0,1 < F_{S12}/F_{S13} < 0,3$

$$\frac{R_2}{R_1} = \frac{a + c\ln\left(\frac{t_{DR1\max}}{M13}\right) + e\ln\left(\frac{F_{S12}}{F_{S13}}\right) + g\left(\ln\left(\frac{t_{DR1\max}}{M13}\right)\right)^2 + i\left(\ln\left(\frac{F_{S12}}{F_{S13}}\right)\right)^2 + k\ln\left(\frac{t_{DR1\max}}{M13}\right)\ln\left(\frac{F_{S12}}{F_{S13}}\right)}{1 + b\ln\left(\frac{t_{DR1\max}}{M13}\right) + d\ln\left(\frac{F_{S12}}{F_{S13}}\right) + f\left(\ln\left(\frac{t_{DR1\max}}{M13}\right)\right)^2 + h\left(\ln\left(\frac{F_{S12}}{F_{S13}}\right)\right)^2 + j\ln\left(\frac{t_{DR1\max}}{M13}\right)\ln\left(\frac{F_{S12}}{F_{S13}}\right)} \tag{39}$$

For $0,3 < F_{S12}/F_{S13} < 0,6$

www.arpnjournals.com

$$\ln\left(\frac{R_2}{R_1}\right) = a + \frac{b}{ln\left(\dfrac{t_{DR1max}}{M13}\right)} + \frac{c}{\left(\dfrac{t_{DR1max}}{M13}\right)} + \frac{d}{\left(\dfrac{t_{DR1max}}{M13}\right)^{(1,5)}} + \frac{e}{\left(\dfrac{t_{DR1max}}{M13}\right)^2}$$

$$+ f\left(\frac{F_{S12}}{F_{S13}}\right) + g\left(\frac{F_{S12}}{F_{S13}}\right)^{(1,5)} + h\left(\frac{F_{S12}}{F_{S13}}\right)^2 + i\left(\frac{F_{S12}}{F_{S13}}\right)^{(2,5)}$$

(40)

For $3,5 \leq R_2/R_1 < 7$:

$$R_2 = R_1\left(\frac{2,6766673 - 0,22589317(t_{DR})_{max} + 0,17183862(M13) - 0,0014327696(M13)^2 + 5,3310075x10^{-6}(M13)^3}{1 - 0,014790427(t_{DR})_{max} - 0,1460338(M13) - 0,0004564009(M13)^2 + 1,523638x10^{-6}(M13)^3}\right)$$

(41)

The permeability of the outer region is found using the following equation:

$$k_3 = \frac{70,6q_a\mu_3 B}{h\left(t*\Delta P'\right)_{r3}}$$

(42)

Table-1. Constants values for Equations (38) to (40).

Coefficient	Equation (38)	Equation (39)	Equation (40)
a	1,148056075	-1,65348167	-123,171636754
b	-0,054300723	0,359685904	-96,912384629
c	-0,1111916097	3,633603633	518,685599496
d	-29,28054451	0,7867843589	-1098,051770102
e	-31,94854034	-0,53215988	1004,175610598
f	0,0085109453	0,011789055	2761,218331423
g	-0,024785904	0,024704553	-7677,7631303581
h	194,799992696	0,140924797	7924,945179820
i	208,154701539	0,18132819	-2877,195951804
j	0,15346215629	0,202918526	-
k	0,84388292168	1,930425704	-

5. EXAMPLES

Example-1

Table-1 contains reservoir and fluid properties for an example presented by Onyekonwu and Ramey (1986). Pressure and pressure derivative data are reported in Figure-9. Characterize the reservoir and estimate the radius of inner and intermediate region.

Solution

The log-log plot of pressure and pressure derivative against injection time is given in Figure-9. From that plot the following information was read:

$t_{r1} = 0,01$ hr $\Delta P_{r1} = 33,83$ psi $(t*\Delta P')_{r1} = 4,1658$ psi
$t_{max} = 427,6$ hr $(t*\Delta P')_{r3} = 4282,033$ psi $t_{er1} = 0,023$ hr

Table-3 presents the results for the examples along with the respective equations. The results are placed in the appropriate order as the parameters are calculated. A deviation error for most of the parameters is also provided.

Table-2. Reservoir and fluid data for examples.

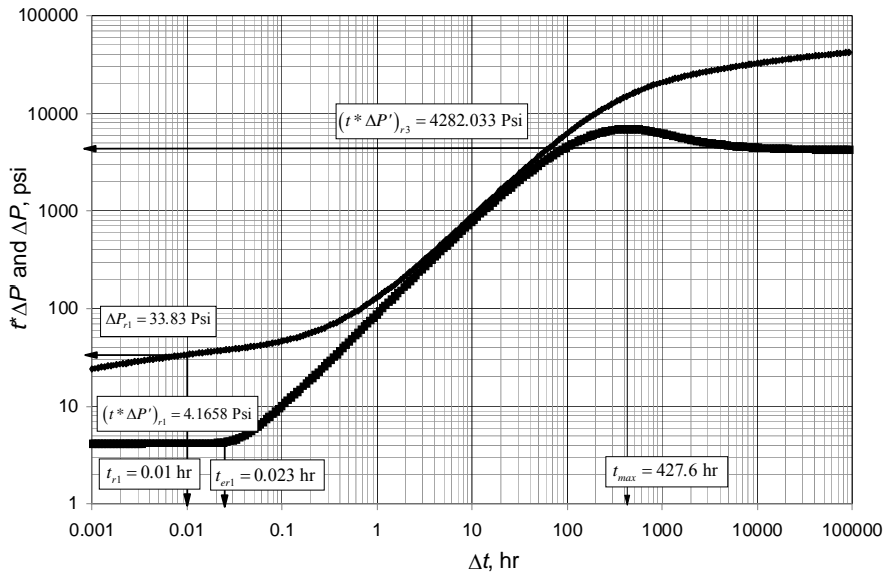| PARAMETER	Example-1	Example-2
q_a, STB/D	100	100
B, bbl/STB	1, 5	1, 2
h, ft	50	50
r_w, ft	0.5	0.5
$(\phi c_t)_1$, 1/psi	$4x10^{-7}$	$4x10^{-7}$
$(\phi c_t)_2$, 1/psi	$8x10^{-8}$	$4x10^{-8}$
$(\phi c_t)_3$, 1/psi	$1, 16x10^{-8}$	$4x10^{-9}$
λ_1, md/cp	50	50
λ_2, md/cp	2	10
λ_3, md/cp	0, 05	2
R_1, ft	68, 5	100
R_2, ft	105	1100

www.arpnjournals.com

Figure-9. Pressure and pressure derivative for example-1.

Example-2

An injection test was simulated using the information from Table-2. Pressure and pressure derivative data are reported in Figure-10. Characterize the reservoir and estimate the radius of inner and intermediate region.

Solution

The log-log plot of pressure and pressure derivative against injection time is given in Figure-10. From that plot the following information was read:

$t_{r1} = 0,01 hr$ $\Delta P_{r1} = 27,2$ psi $(t*\Delta P')_{r1} = 3,34$ psi
$t_{max2} = 235 hr$ $(t*\Delta P')_{max2} = 130,4$ psi $(t*\Delta P')_{r3} = 85,45$ psi
$t_{er1} = 0,054 hr$

As for example-1, Table-3 also presents the results for example-2 along with the respective equations.
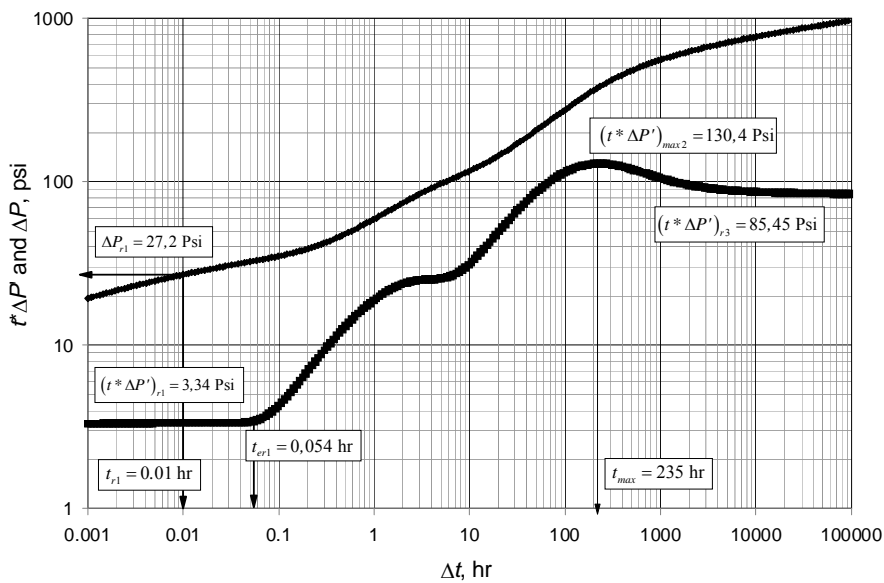

Figure-10. Pressure and pressure derivative for example-2.

www.arpnjournals.com

Table-3. Results of examples.

Parameter	Equation	Example-1	% error	Example-2	% error
$(k/\mu)_1$, md/cp	23	50,84	1,7	50,73	1,46
s	24	0,055	-	0,067	-
R_1, ft	25	65,44	4,5	100,17	0,17
$(k/\mu)_3$, md/cp	42	0,049	2	1,98	1
F_{S12}	21	5	0	10	0
F_{S13}	22	34,483	0,0007	100	0
M_{13}	20	1037,55	3,75	25,62	2.48
$(k/\mu)_2$, md/cp	33	-	-	11,7	17
M_{12}	19	-	-	4,33	13.4
R_2, ft	38	111,38	6,07	1161.8	5.31

ANALYSIS OF RESULST

As observed in Table-3, the estimated parameters are very acceptable with absolute deviation errors even of zero. For the second exercise, the estimated mobility of region 2 is 11, 7 md/cp. If compared with the actual value of 10 md/cp, it falls into an adequate range although the absolute error is 17%. Most of the values agree certainly well with the expected results indicating that the developed equations are useful.

CONCLUSIONS

Pressure derivative behavior for three-region composite reservoirs with mobility and storativity ratio contrast was studied and a methodology to estimate the distance inner and intermediate regions and mobility ratios were introduced and successfully tested with synthetic examples. Comparing to the actual values, the estimated parameters fall into an adequate range of values this indicates that the provided equation are well developed.

ACKNOWLEDGMENTS

Nomenclature

B	FVF, rb/STB
c_t	System total compressibility, 1/psi
F_s	Storativity ratio
h	Formation thickness, ft
k	Permeability, md
M	Mobility ratio
p	Pressure, psi
q_a	Flow/injection rate, STB/D
R	Discontinuity Radius, ft
r	Radius, ft
s	Skin Factor
t	Time, hr
t_{DR}	Dimensionless time based on R
$t*\Delta p'$	Pressure derivative, psi

Greeks

Δ	Change, drop
ϕ	Porosity, Fraction
μ	Viscosity, cp
λ	Mobility, md/cp

www.arpnjournals.com

Suffices

1	Inner region
2	Intermediate region
3	Outer region
D	Dimensionless
max	Maximum dimensionless pressure derivative or time
w	Wellbore

REFERENCES

Ambastha A.K. and Ramey Jr. H.J. 1989. Thermal Recovery Well Test Design and Interpretation. SPE Formation Evaluation. 4(2): 173-180.

Ambastha A.K. and Ramey Jr. H.J. 1992. Pressure Transient Analysis for a Three-Region Composite Reservoir. SPE 24378 SPE Rocky Mountain Regional Meeting, Casper, Wyoming, U.S.A. 18-21 May.

Barua J. and Horne R.N. 1987. Computerized Analysis of Thermal Recovery Well Test Data. SPE Formation Evaluation. 2(4): 560-566.

Brown L.P. 1985. Pressure Transient Behavior of the Composite Reservoir. SPE 14316 SPE Annual Technical Conference and Exhibition, Las Vegas, Nevada, U.S.A. 22-25 September.

Escobar F.H., Martínez J.A. and Bonilla L.F. 2011. Pressure and Pressure Derivative Analysis Without Type-curve matching for Thermal Recovery Process. CT and F - Ciencia, Tecnología y Futuro. 4(4): 23-35.

Gates C.F. and Ramey H.J. Jr. 1978. Engineering of In-situ Combustion Oil Recovery Projects. SPE 7149 48th California Regional Meeting, San Francisco, California, U.S.A. 12-14 April.

Onyekonwu M.O. 1985. Interpretation of In-Situ Combustion Thermal Recovery Falloff Tests. Ph.D. Dissertation. Stanford University, California.

Satman A., Eggenschwiler M. and Ramey H. Jr. 1980. Interpretation of Injection Well Pressure Transient Data in Thermal Oil Recovery. SPE 8908 SPE California Regional Meeting, Los Angeles, California, U.S.A. 9-11 April.

Tiab D. 1993. Analysis of Pressure and Pressure Derivative without Type-Curve Matching: 1- Skin and Wellbore Storage. Journal of Petroleum Science and Engineering. 12: 171-181.

Walsh Jr. John W., Ramey Jr. H.J. and Brigham W.E. 1981. Thermal Injection Well Falloff Testing. SPE 10227 SPE Annual Technical Conference and Exhibition, San Antonio, Texas, U.S.A. 4-7 October.

Watenbarger R.A. and Ramey H.J. Jr. 1970. An Investigation of Wellbore Storage and Skin Effects in Unsteady Liquid Flow: II. Finite Difference Treatment. SPEJ. pp. 291-297.